Derivative properties from high-precision equations of state

THE JOURNAL OF PHYSICAL CHEMISTRY B

Article

pubs.acs.org/JPCB

Derivative Properties from High-Precision Equations of State

Reza Haghbakhsh,[†] Morten Konttorp,[‡] Sona Raeissi,[†] Cor J. Peters,*[,§,∥] and John P. O'Connell[⊥]

[†]School of Chemical and Petroleum Engineering, Shiraz University, Mollasadra Avenue, Shiraz 71345, Iran

[‡]Delft University of Technology, Stevinweg 1, 2628 CN Delft, The Netherlands

[§]Department of Chemical Engineering and Chemistry, Separation Technology Group, Eindhoven University of Technology, Den Dolech 2, 5612 AZ Eindhoven, The Netherlands

[∥]Chemical Engineering Department, The Petroleum Institute, P.O. Box 2533, Abu Dhabi, United Arab Emirates

[⊥]Department of Chemical Engineering, University of Virginia, Charlottesville, Virginia 22901, United States

Supporting Information

ABSTRACT: In this study, the behavior of derivative properties estimated by equations of state, including isochoric heat capacity, isobaric heat capacity, speed of sound, and the Joule−Thomson coefficient for pure compounds and a mixture, has been investigated. The Schmidt−Wagner and Jacobsen−Stewart equations of state were used for predictions of derivative properties of 10 different pure compounds from various nonpolar hydrocarbons, nonpolar cyclic hydrocarbons, polar compounds, and refrigerants. The estimations were compared to experimental data. To evaluate the behavior of mixtures, the extended corresponding states principle (ECS) was studied. Analytical relationships were derived for isochoric heat capacity, isobaric heat capacity, the Joule−Thomson coefficient, and the speed of sound. The ECS calculations were compared to the reference surface data of methane + ethane. The ECS principle was found to generate data of high quality.

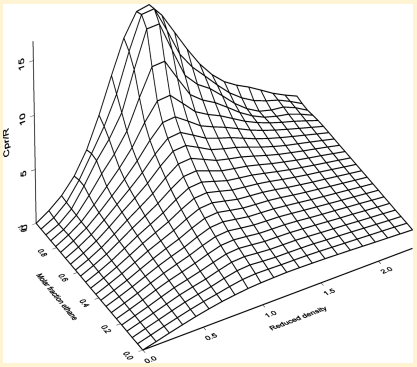

1. INTRODUCTION

Nowadays, energy is among the most important global concerns. Most of the energy consumed in the world comes from petroleum sources.[1] Efficient process design and intensification are among the various paths to alleviate such problems. However, optimal design requires accurate knowledge of the various thermophysical properties of the pure components involved in the processes, and their mixtures. This includes second-order thermodynamic derivative properties, such as heat capacities, speeds of sound, and Joule−Thomson coefficients, as well as the first-order properties.[2,3] For example, heat capacities are properties of high interest in any process involving the addition or extraction of heat, and the Joule−Thomson coefficients are essential for engineering designs such as throttling processes. The speed of sound is commonly employed for aerodynamic calculations.[4,5] These thermodynamic properties can be calculated by second-order differentiation of a thermodynamic potential function with respect to the temperature and density.[4]

However, calculations of second derivatives are more sensitive to errors than the first derivatives of a thermodynamic function. First derivatives, such as phase equilibria calculations, come to rather accurate results, whereas second derivatives of the same thermodynamic function can lead to unreliable results for the same compound.[5] It has been pointed out that this is a challenge for all equations of state. For example, cubic equations of state (EoS) have proven to be rather accurate models for first derivatives; however, they have problems with predicting some of the singularities observed in derivative properties, for instance, density extrema in isothermal variations of the isochoric heat capacity, isothermal compressibility, and speed of sound.[6] Hence, such equations have little predictive or extrapolative power.[5]

For overcoming this inability of the cubic EoS, some researchers have used more complicated EoS, involving more sophisticated molecular interactions, or EoS that involve a greater number of parameters. For example, the SAFT-family of EoS or the cubic-plus-association (CPA) EoS are the choices for some researchers when it comes to prediction of second derivative properties, despite the fact that they are cumbersome to use.[2,3,5,7−9]

In this study, other sophisticated EoS, namely, the Schmidt−Wagner and the Jacobsen−Stewart (32-MBWR) EoS, were considered as accurate models to predict second derivative properties of pure fluids, as well as mixtures. These EoS have larger numbers of parameters compared to the cubic EoS and even compared to the SAFT-family of equations; however, most importantly, they have a strong thermodynamic basis.

2. THEORY

2.1. Equations of State. In this section, the functional structure of the investigated equations of state, namely, the Schmidt−Wagner (SW) EoS and the Jacobsen−Stewart EoS

Received: August 19, 2014
Revised: October 17, 2014
Published: October 27, 2014

Table 1. Definition of Dimensionless Variables

dimensionless variable	relation
ideal Helmholtz energy	$\Phi^0 = \frac{A^{id}}{RT}$
residual Helmholtz energy	$\Phi^r = \frac{A - A^{id}}{RT}$
dimensionless temperature	$\tau = \frac{T_c}{T}$
dimensionless density	$\delta = \frac{\rho}{\rho_c}$

(32-MBWR), will be discussed for both pure compounds and mixtures.

2.1.1. Schmidt–Wagner EoS. In 1985, Schmidt and Wagner[10] published an equation of state for oxygen, based on a new method of optimization. They developed their new EoS based on four goals, as follows: (1) The equation of state should be able to simultaneously fit all kinds of measured thermodynamic data in order to represent all types of properties within experimental accuracy. (2) The equation should be able to cover the whole fluid region where data exist. (3) It should have a simple functional form and be simple to handle. (4) To minimize the number of coefficients, the structure of the new equation of state should be developed using an optimization method.

The fundamental equation obtained was expressed in the form of the Helmholtz energy, A, with two independent variables, density (ρ) and temperature (T). Therefore, derivative properties could be derived based on this equation of state.[10] The dimensionless Helmholz energy ($\Phi = A/RT$) is split into a part presenting ideal gas behavior, Φ°, and a part that takes into account the residual fluid behavior, Φ^r.

$$\Phi(\delta, \tau) = \Phi^0(\delta, \tau) + \Phi^r(\delta, \tau) \quad (1)$$

The parameters of eq 1 are defined in Table 1.

The Helmholz energy of an ideal gas is given by

$$A^0(\rho, T) = H^0(T) - RT - TS^0(\rho, T) \quad (2)$$

If the ideal gas heat capacity, C_p^0, is known, the following equation is obtained,

$$A^0(\rho, T) = \int_{T_0}^{T} C_p^0 \, dT + H_0^0 - RT - T\int_{T_0}^{T} \frac{C_p^0 - R}{T} dT - RT\ln\left(\frac{\rho}{\rho_c}\right) - TS_0^0 \quad (3)$$

where $\rho_0 = (P_0/RT_0)$ is a reference density. Furthermore, arbitrary reference values for the temperature T_0, pressure P_0, entropy S_0^0, and enthalpy H_0^0 have to be selected. The development of the residual term of the Helmholz energy, Φ^r, is split into three steps:

Step 1. The first step is the formulation of a general expression for the equation that functions as a "bank of terms". For methane,

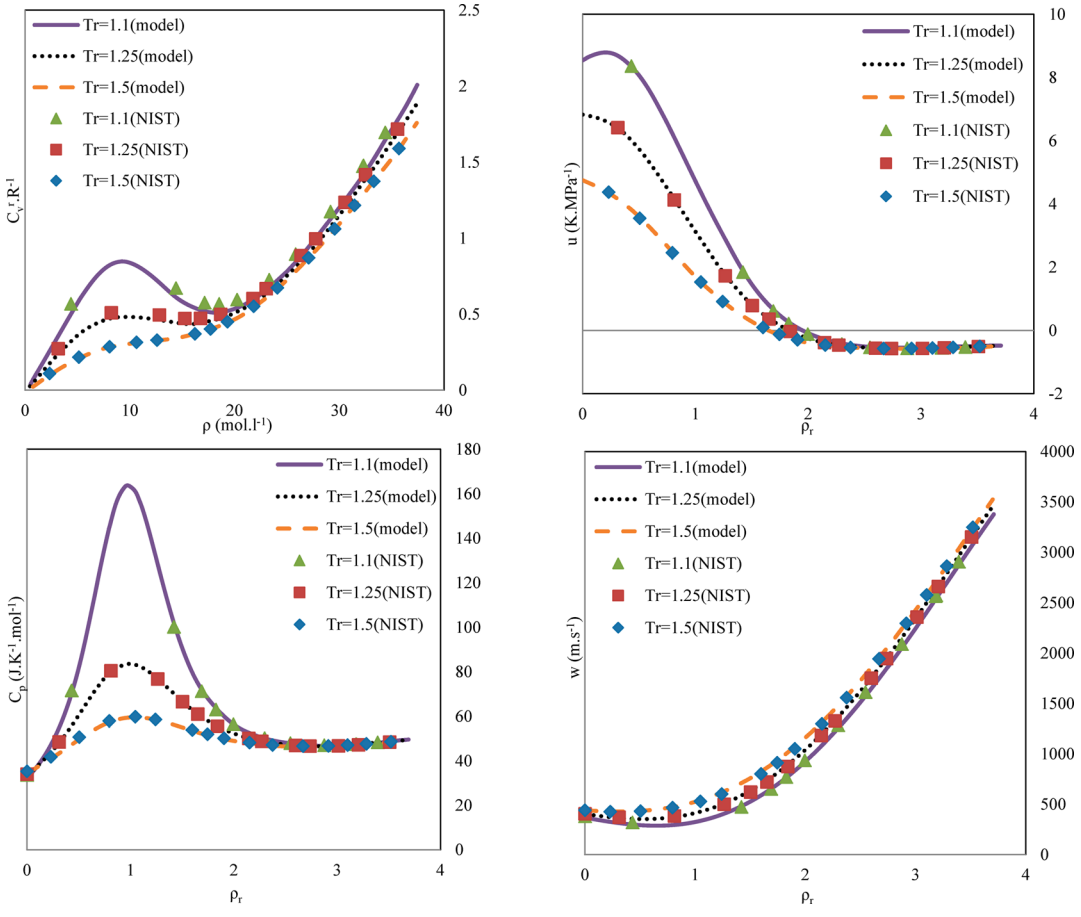

Figure 1. Derived thermodynamic properties for methane by the Schmidt–Wagner EoS and comparison with NIST[16] data at different reduced temperatures.

dx.doi.org/10.1021/jp508357f | J. Phys. Chem. B 2014, 118, 14397–14409

and similar components, this residual part of the dimensionless Helmholz energy was formulated as

$$\Phi^{r}(\delta, \tau) = \sum_{i=1}^{10}\sum_{j=-1}^{9} n_i \delta^i \tau^{j/2} + e^{-\delta}\sum_{i=1}^{6}\sum_{j=0}^{5} n_i \delta^i \tau^j + e^{-\delta^2}\sum_{i=1}^{7}\sum_{j=0}^{10} n_i \delta^i \tau^j + e^{-\delta^3}\sum_{i=1}^{3}\sum_{j=0}^{13} n_i \delta^i \tau^{2j} + e^{-\delta^4}\sum_{i=1}^{6}\sum_{j=5}^{11} n_i \delta^i \tau^{2j} + e^{-\delta^5}\sum_{i=1}^{3}\sum_{j=7}^{13} n_i \delta^i \tau^j + (e^{-0.4\delta^6} - e^{-2\delta^6})\sum_{i=3}^{6}\sum_{j=10}^{15} n_i \delta^i \tau^{2j} + \sum_{i=1}^{27} n_i \delta^{di} \tau^{ti} e^{-a_i(\delta-\Delta_i)^2 - \beta_i(\tau-\gamma_i)^2} \quad (4)$$

where

$$\Delta = \theta^2 + B_k[(\delta - 1)^2]^{a_i}, \quad \theta = (1 - \tau) + A[(\delta - 1)^2]^{1/2\beta} \quad (5)$$

and

$$\tau = \frac{T_c}{T}, \quad \delta = \frac{\rho}{\rho_c} \quad (6)$$

All of the other symbols represent constants that are fit to experimental data.

Step 2. The second step, after selecting a suitable bank of terms, is a statistical optimization to determine the most effective equation for Φ^r. This will consist of the terms from eq 4 that give the best representation of the data.

Step 3. The third step is the optimization of the parameters, n_i's, in the obtained equation. In the optimization of the parameters, the following information is used: p, ρ, and T data, isochoric heat capacities, isobaric heat capacities, second virial coefficients, speeds of sound, enthalpies, vapor pressures, vapor densities, and liquid densities.

Steps 2 and 3 are repeated until the best equation and the best parameter set are found. In the literature, three types of SW EoS are mentioned. The methane-type of SW EoS was already discussed. The other equations of state are the oxygen-type and the carbon dioxide-type. The differences are in the banks of terms. For the methane-type of SW EoS, some extra terms are included in the bank of terms to give a better fit in the critical region.[10]

2.1.2. Jacobsen−Stewart (32-MBWR) EoS. The Jacobsen−Stewart (32-MBWR) EoS[11] is a modification of the Benedict−Webb−Rubin EoS. The 32-MBWR equation consists of an exponential term that is essentially an expanded virial equation. This equation is capable of providing highly accurate fits of the liquid, vapor, and supercritical regions of a fluid, as well as the saturation boundary. The 32-MBWR equation presents pressure (P) as a function of molar density (ρ) and temperature (T),

$$P(\rho, T) = \sum_{i=1}^{9} a_i(T)\rho^i + \exp(-\delta^2)\sum_{i=10}^{15} a_i(T)\rho^{2i-17} \quad (7)$$

where $\delta = (\rho/\rho_c)$ and the temperature dependencies of the a_i coefficients are

Table 2. Compounds, from Different Classes of Families, Investigated in This Study

type of compound	compound
nonpolar hydrocarbons	methane
	ethane
	propane
	i-butane
	n-butane
nonpolar cyclic hydrocarbons	cyclohexane
refrigerants	**R152a** (1,1-difluoroethane)
	sulphurhexafluoride
polar compounds	methanol
	water

$$a_1 = RT$$

$$a_2 = b_1 T + b_2 T^{0.5} + b_3 + \frac{b_4}{T} + \frac{b_5}{T^2}$$

$$a_3 = b_6 T + b_7 + \frac{b_8}{T} + \frac{b_9}{T^2}$$

$$a_4 = b_{10} T + b_{11} + \frac{b_{12}}{T}$$

$$a_5 = b_{13}$$

$$a_6 = \frac{b_{14}}{T} + \frac{b_{15}}{T^2}$$

$$a_7 = \frac{b_{16}}{T}$$

$$a_8 = \frac{b_{17}}{T} + \frac{b_{18}}{T^2}$$

$$a_9 = \frac{b_{19}}{T^2}$$

$$a_{10} = \frac{b_{20}}{T^2} + \frac{b_{21}}{T^3}$$

$$a_{11} = \frac{b_{22}}{T^2} + \frac{b_{23}}{T^4}$$

$$a_{12} = \frac{b_{24}}{T^2} + \frac{b_{25}}{T^3}$$

$$a_{13} = \frac{b_{26}}{T^2} + \frac{b_{27}}{T^4}$$

$$a_{14} = \frac{b_{28}}{T^2} + \frac{b_{29}}{T^3}$$

$$a_{15} = \frac{b_{30}}{T^2} + \frac{b_{31}}{T^3} + \frac{b_{32}}{T^4} \quad (8)$$

where the coefficients of b are the adjustable parameters.[11]

2.1.3. General Comparisons of the 32-MBWR and SW EoS. In general, the complexity of calculations of derivative properties depends on the number of terms used in the EoS. The 32-MBWR EoS has a larger number of terms than the SW EoS, but all the derivative properties can still be obtained by means of analytic differentiation. The SW EoS usually has more parameters than the 32-MBWR (depending on the optimization of the functional structure). Because the thermodynamic surface

dx.doi.org/10.1021/jp508357f | J. Phys. Chem. B 2014, 118, 14397−14409

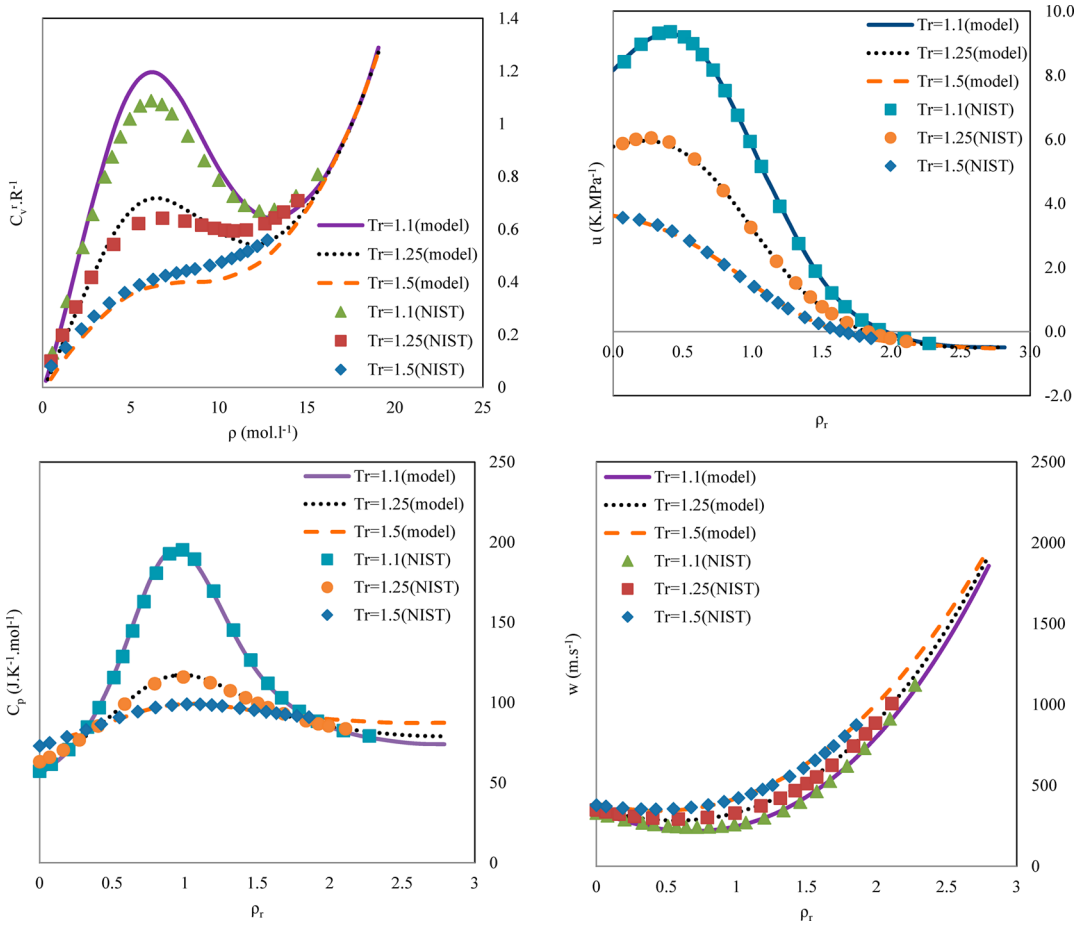

Figure 2. Derived thermodynamic properties for ethane by the 32MBWR EoS and comparison with NIST[16] data at different reduced temperatures.

is given as the free Helmholtz energy as a function of density and temperature, more complex differentiations have to be conducted to obtain the derivative properties. The derivative properties are, however, still obtained by means of analytic differentiation.

2.2. Derivation of Derivative Properties for Pure Compounds. If the thermodynamic surface is given as a function of temperature and density, the basic relations giving the derivatives of the Helmholtz free energy in a dimensionless form are as follows, with the dimensionless variables being defined in Table 1.

$$\Phi_{\tau}^{r} = \left(\frac{d\Phi^{r}}{d\tau}\right)_{\delta} \tag{9.1}$$

$$\Phi_{\tau\tau}^{r} = \left(\frac{d^2\Phi^{r}}{d\tau^2}\right)_{\delta} \tag{9.2}$$

On the basis of the Helmholtz energy, different derivative properties such as isochoric heat capacity, C_v; isobaric heat capacity, C_p; speed of sound, w; and Joule−Thomson coefficient, μ, can be derived, and the final equations for the Schmidt−Wagner EoS are as follows.

$$\frac{C_v(\delta, \tau)}{R} = -\tau^2(\Phi_{\tau\tau}^{0} + \Phi_{\tau\tau}^{r}) \tag{10.1}$$

$$\frac{C_p(\delta, \tau)}{R} = \frac{C_v(\delta, \tau)}{R} + \frac{(1 + \delta\Phi_{\delta}^{r} - \delta\tau\Phi_{\delta\tau}^{r})^2}{1 + 2\delta\Phi_{\delta}^{r} + \delta^2\Phi_{\delta\delta}^{r}} \tag{10.2}$$

$$\frac{w^2(\delta, \tau)}{RT} = 1 + 2\delta\Phi_{\delta}^{r} + \delta^2\Phi_{\delta\delta}^{r} - \frac{(1 + \delta\Phi_{\delta}^{r} - \delta\tau\Phi_{\delta\tau}^{r})^2}{\tau^2(\Phi_{\tau\tau}^{0} + \Phi_{\tau\tau}^{r})} \tag{10.3}$$

$$\mu(\delta, \tau)R\rho = \frac{-(\delta\Phi_{\delta}^{r} + \delta^2\Phi_{\delta\delta}^{r} + \delta\tau\Phi_{\delta\tau}^{r})}{(1 + \delta\Phi_{\delta}^{r} - \delta\tau\Phi_{\delta\tau}^{r})^2 - \tau^2(\Phi_{\tau\tau}^{0} + \Phi_{\tau\tau}^{r})(1 + 2\delta\Phi_{\delta}^{r} + \delta^2\Phi_{\delta\delta}^{r})} \tag{10.4}$$

Equations 10 are the derived thermodynamic properties as a function of dimensionless Helmholtz energy. If the thermodynamic surface is given in pressure as a function of density and temperature, such as the 32-MBWR EoS, the basic thermodynamic relations are as follows.

$$C_v(\rho, T) = C_v^{0} - \int_0^{\rho}\left[\frac{T}{\rho^2}\left(\frac{\partial^2 P}{\partial T^2}\right)_{\rho}\right]d\rho \tag{11.1}$$

$$C_p(\rho, T) = C_v(\rho, T) + \frac{T}{\rho^2}\left(\frac{\partial P}{\partial T}\right)_{\rho}^{2}\Bigg/\left(\frac{\partial P}{\partial \rho}\right)_{T} \tag{11.2}$$

$$w^2(\rho, T) = \left[\frac{C_p}{C_v}\left(\frac{\partial P}{\partial \rho}\right)_{T}\frac{10^6}{M_r}\right] \tag{11.3}$$

$$\mu(\rho, T) = \frac{1}{C_p}\left[\frac{T(\partial P/\partial T)_{\rho}}{\rho^2(\partial P/\partial \rho)_{T}} - \frac{1}{\rho}\right] \tag{11.4}$$

dx.doi.org/10.1021/jp508357f | J. Phys. Chem. B 2014, 118, 14397−14409

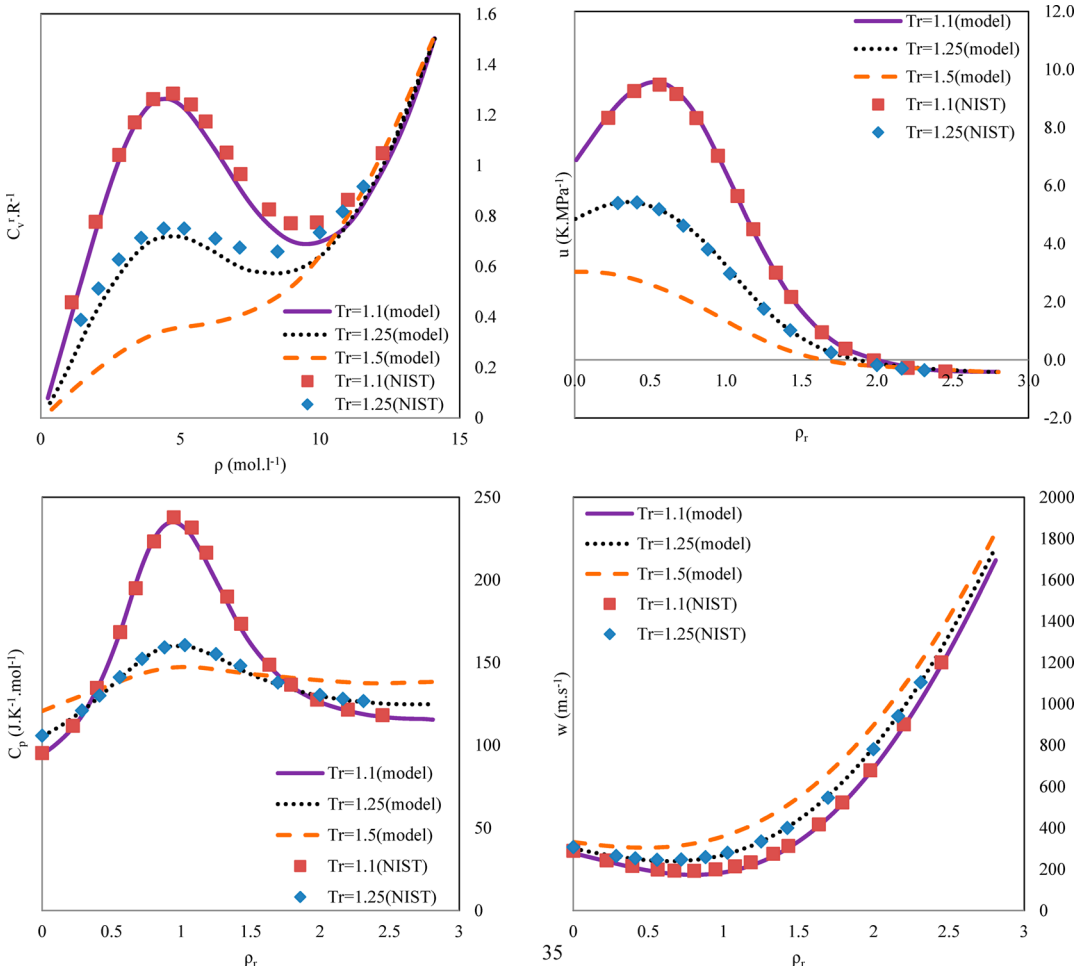

Figure 3. Derived thermodynamic properties for propane by the 32MBWR EoS and comparison with NIST[16] data at different reduced temperatures.

The residual properties can be derived via a straightforward procedure. Values of residual heat capacity are useful to determine, as they can, for example, reveal deviations in the isochoric heat capacity. The advantage of comparing the residual heat capacities is that the dependence on the ideal heat capacity is removed. The residual heat capacity is given by eq 12,

$$\frac{C_v^{\mathrm{r}}}{R} = -\frac{1}{R}\int_0^{\rho} \frac{T}{\rho^2}\left(\frac{\mathrm{d}^2 P}{\mathrm{d}T^2}\right)_{\rho} \mathrm{d}\rho \tag{12}$$

To study the isobaric heat capacity, without the influence of the isochoric heat capacity, the following relation is used,

$$\frac{C_p^{\mathrm{r}} - C_v^{\mathrm{r}}}{R} = \frac{T}{R\rho^2}\left(\frac{\mathrm{d}P}{\mathrm{d}T}\right)_{\rho}^2 \Big/ \left(\frac{\mathrm{d}P}{\mathrm{d}\rho}\right)_T - 1 \tag{13}$$

This property has the advantage that the deviations in C_v and the ideal isobaric heat capacity are not influencing the comparison. To study the total isobaric heat capacity, the residual isobaric heat capacity is included. Note that this quantity is not dependent on the ideal isobaric heat capacity.

$$\frac{C_p^{\mathrm{r}}}{R} = \frac{C_v^{\mathrm{r}}}{R} + \frac{T}{R\rho^2}\left(\frac{\mathrm{d}P}{\mathrm{d}T}\right)_{\rho}^2 \Big/ \left(\frac{\mathrm{d}P}{\mathrm{d}\rho}\right)_T - 1 \tag{14}$$

To compare the Joule−Thomson coefficient with eq 11.4, the dependence on the isobaric heat capacity is discarded, yielding the following expression:

$$\mu C_p \rho = \frac{T\left(\frac{\mathrm{d}P}{\mathrm{d}T}\right)_{\rho}}{\rho\left(\frac{\mathrm{d}P}{\mathrm{d}\rho}\right)_T} - 1 \tag{15}$$

The experimentally based values of C_v^{r}/R for comparison with those estimated by EoS can be obtained as

$$\frac{C_v^{\mathrm{r}}}{R} = \frac{C_v}{R} - \frac{C_v^{\mathrm{ig}}}{R} \tag{16}$$

$$C_p^{\mathrm{ig}} - C_v^{\mathrm{ig}} = R \tag{17}$$

Values of C_p^{ig}/R were calculated for the compounds based on the following correlation:[12]

$$\frac{C_p^{\mathrm{ig}}}{R} = a_0 + a_1 T + a_2 T^2 + a_3 T^3 + a_4 T^4 \tag{18}$$

2.3. Calculation of Derivative Properties for Mixtures.

2.3.1. Extended Corresponding States Procedure. To calculate the derivative properties for mixtures, the extended corresponding states (ECS) procedure is chosen.[13−15] This procedure allows an accurate calculation of all thermodynamic properties provided that there are accurate pure component surfaces

dx.doi.org/10.1021/jp508357f | J. Phys. Chem. B 2014, 118, 14397−14409

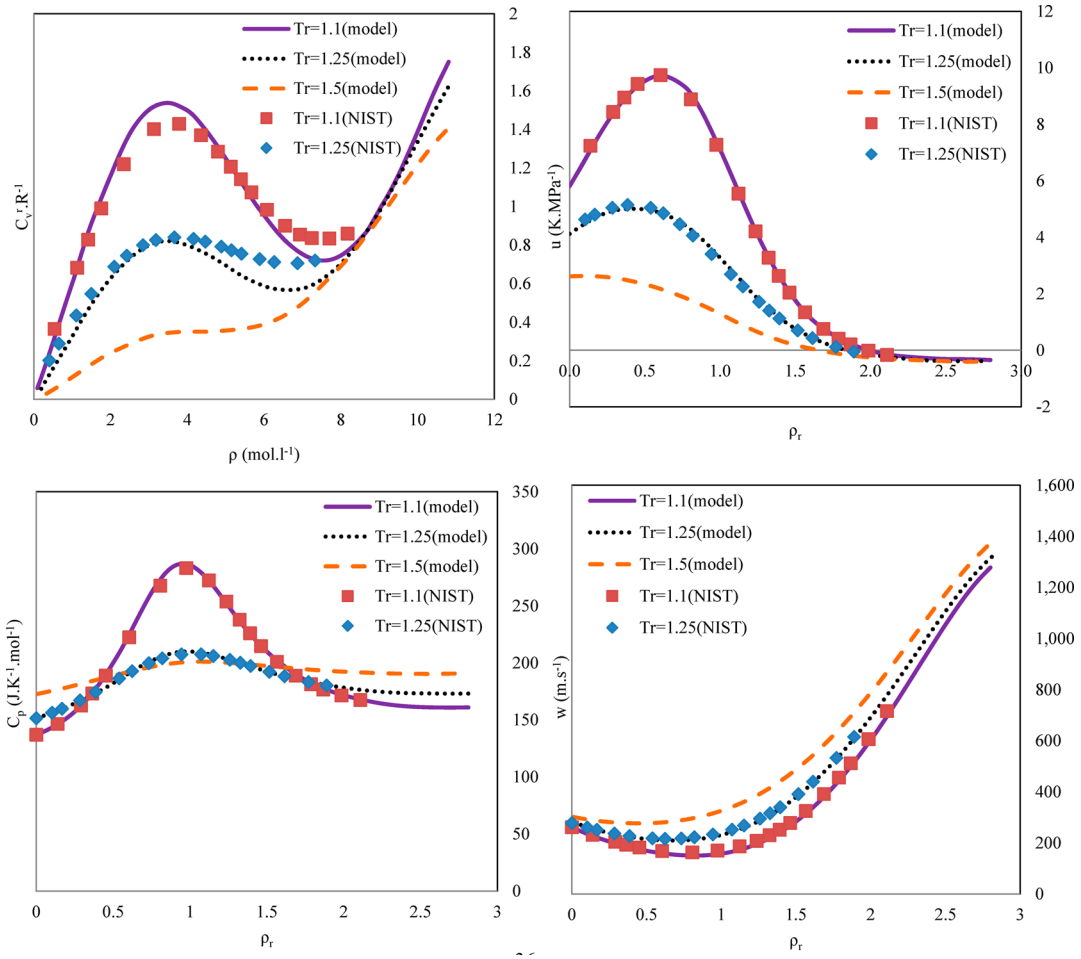

Figure 4. Derived thermodynamic properties for i-butane by the 32MBWR EoS and comparison with NIST[16] data at different reduced temperatures.

available. The extended corresponding states method is based on the following relationships:[14]

$$z_i(\rho, T) = z_0(\rho_i h_{i,0}, T/f_{i,0}) \tag{19}$$

$$a_i(\rho, T) = a_0(\rho_i h_{i,0}, T/f_{i,0}) \tag{20}$$

The subscripts denote the reference fluid (0) and target fluid (i). Z and a are the compressibility factor and the dimensionless residual Helmholtz free energy, respectively, and are defined by

$$z = Z - 1 \tag{21}$$

$$a = \frac{A - A^{\mathrm{id}}}{RT} \tag{22}$$

$f_{i,0}$ and $h_{i,0}$ are transformation parameters, defined by

$$f_{i,0} = (T_c^i/T_c^0)\theta(T_r^i, \rho_r^i) \tag{23}$$

$$h_{i,0} = (\rho_c^0/\rho_c^i)\phi(T_r^i, \rho_r^i) \tag{24}$$

where T_c and ρ_c are the critical temperature and critical molar density of the fluids, respectively. T_r^i and ρ_r^i are defined as

$$T_r^i = \frac{T^i}{T_c^i} \tag{25}$$

$$\rho_r^i = \frac{\rho^i}{\rho_c^i} \tag{26}$$

The functions $\phi(T_r, \rho_r)$ and $\theta(T_r, \rho_r)$ are shape factors. Given a state point defined by ρ and T, plus the transformation variables, $f_{i,0}$ and $h_{i,0}$, eqs 19 and 20 define an exact transformation from one pure fluid surface to another; then, the pressure P_i transfers to $(f_{i,0}/h_{i,0})P_0$. The shape factors $\phi(T_r, \rho_r)$ and $\theta(T_r, \rho_r)$ can be approximated in a number of ways, but if the equation of state is known for both the reference fluid (0) and the target fluid (i), the exact calculation of $h_{i,0}$ and $f_{i,0}$ is possible for each state point. This eliminates the need to approximate $\phi(T_r, \rho_r)$ and $\theta(T_r, \rho_r)$. In this study, the transformation parameters $f_{i,0}$ and $h_{i,0}$ were calculated in an exact manner for every state point. The extension of this procedure to mixtures is accomplished by the following mixing rules,[13]

$$f_{ij} = \varepsilon_{i,j}(f_{ii,0}f_{jj,0})^{1/2} \tag{27}$$

$$h_{ij} = \eta_{i,j}\left(\frac{1}{2}h_{ii,0}^{\ 1/3} + \frac{1}{2}h_{jj,0}^{\ 1/3}\right)^3 \tag{28}$$

$$h_{x,0} = \sum_i \sum_j x_i x_j h_{ij,0} \tag{29}$$

$$f_{x,0}h_{x,0} = \sum_i \sum_j x_i x_j f_{ij,0} h_{ij,0} \tag{30}$$

where x_i and x_j are the mole fractions of the pure components and η_{ij} and ε_{ij} are binary interaction parameters. The previously defined parameters $h_{i,0}$ and $f_{i,0}$ become $h_{ii,0}$ and $f_{ii,0}$, respectively.

dx.doi.org/10.1021/jp508357f | J. Phys. Chem. B 2014, 118, 14397−14409

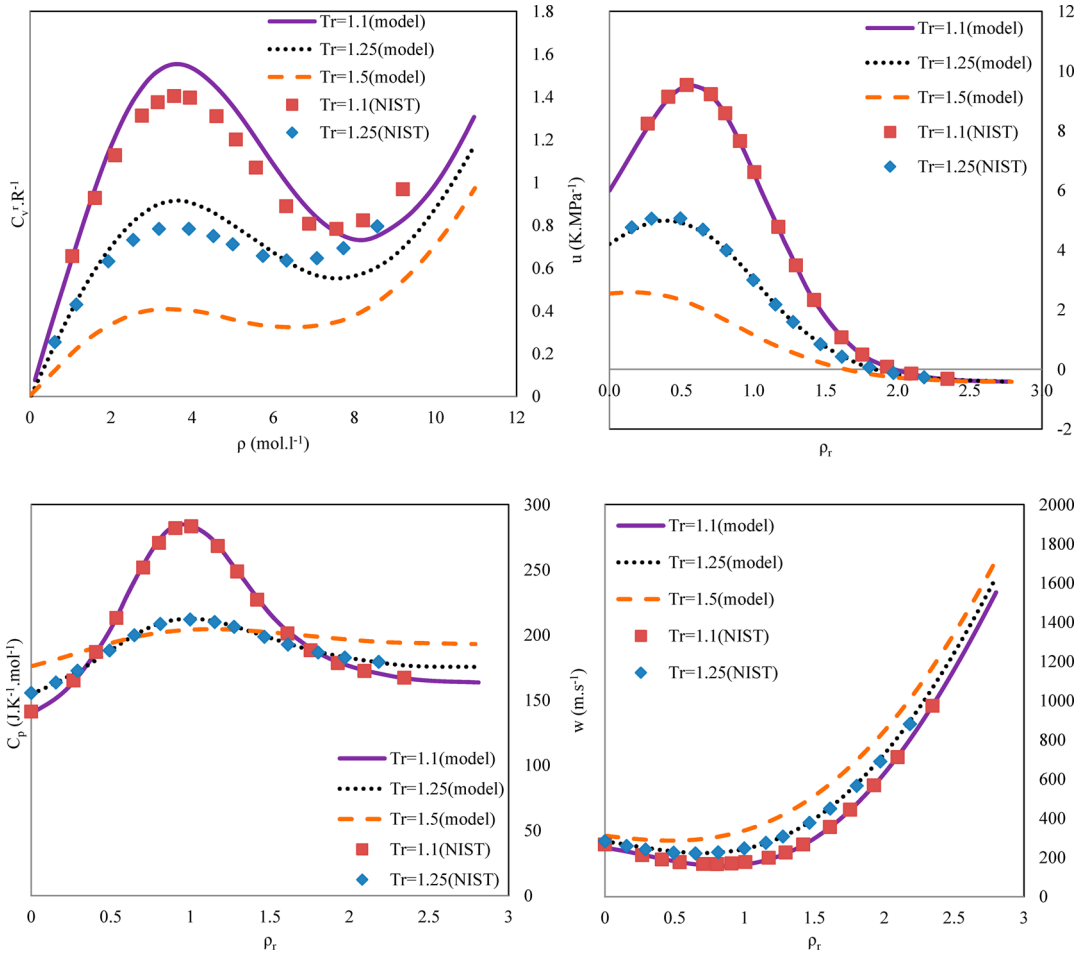

Figure 5. Derived thermodynamic properties for *n*-butane by the 32MBWR EoS and comparison with NIST[16] data at different reduced temperatures.

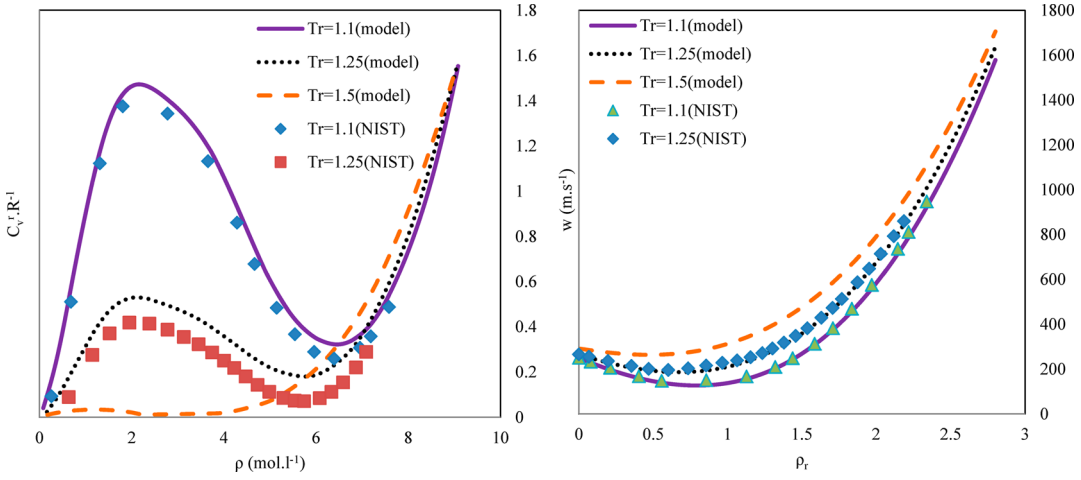

Figure 6. Derived thermodynamic properties for cyclohexane by the Schmidt−Wagner EoS and comparison with NIST[16] data at different reduced temperatures.

The only adjustable parameters are the binary interaction parameters η_{ij} and ε_i.[13,14]

2.3.2. Derivation of Derivative Properties Using the ECS Procedure. Starting with the dimensionless Helmholtz energy, the thermodynamic properties can be derived using basic thermodynamic relationships. Equations 31−37 require only first derivatives of the Helmholtz energy *a*.

$$a_i = a_0 \tag{31}$$

$$z_i = (1 + H_\rho)z_0 + F_\rho u_0 \tag{32}$$

$$u_i = (1 - F_T)u_0 - H_T z_0 \tag{33}$$

$$s_i = s_0 - F_T u_0 - H_T z_0 \tag{34}$$

$$h_i = h_0 + (F_\rho - F_T)u_0 + (H_\rho - H_T)z_0 \tag{35}$$

dx.doi.org/10.1021/jp508357f | J. Phys. Chem. B 2014, 118, 14397−14409

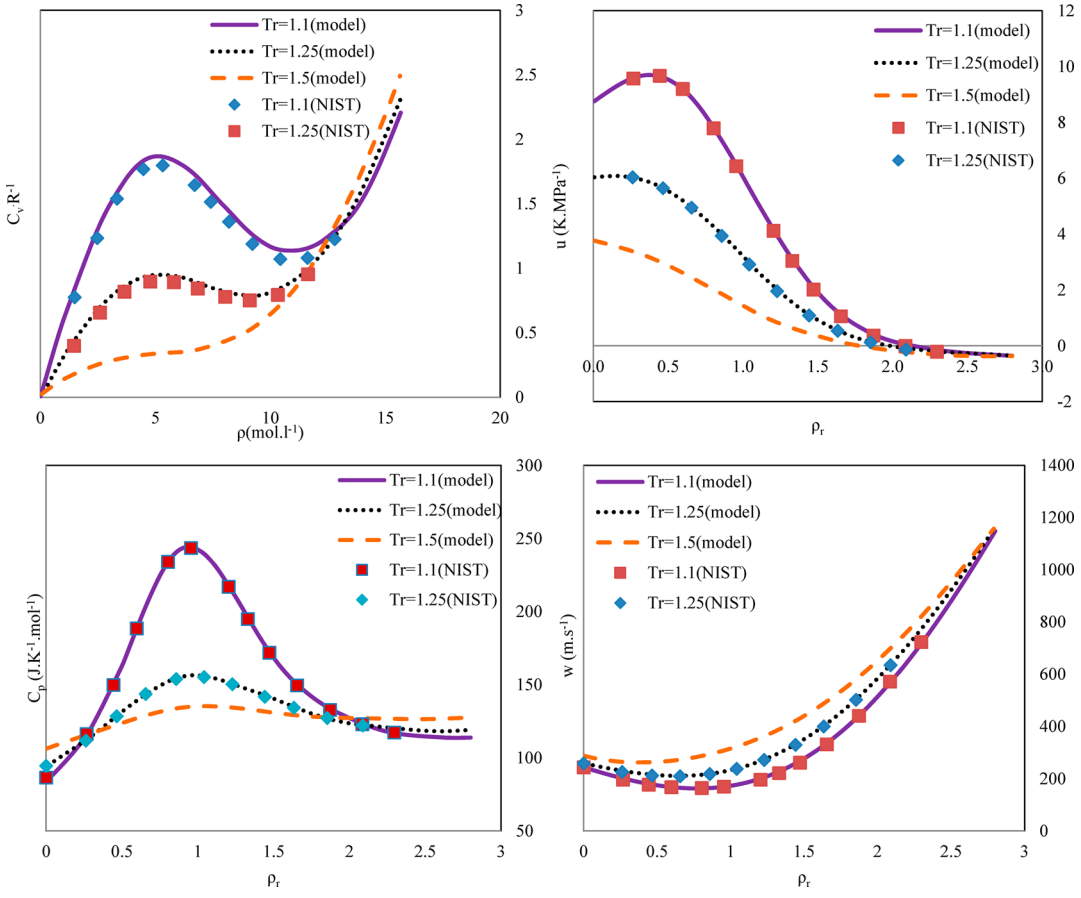

Figure 7. Derived thermodynamic properties for **R152a** by the 32MBWR EoS and comparison with NIST[16] data at different reduced temperatures.

$$g_i = g_0 + H_\rho z_0 + F_\rho u_0 \tag{36}$$

$$\ln \varphi_i = g_0 + u_0 F_{n_i} + z_0 H_{n_i} \tag{37}$$

All energies are defined as

$$x = \frac{X - X^{id}}{RT} \tag{38}$$

where $X = a$, u, h, or g. The entropy is defined as

$$s = \frac{S - S^{id}}{R} \tag{39}$$

The thermodynamic properties denoted with a subscript 0 are properties derived from the reference surface using basic thermodynamic relationships. The factors H_x and F_x (where $x = T$, ρ, or n_i) contain the derivatives of the transformation parameters $h_{i,0}$ and $f_{i,0}$. Their definitions are

$$F_T = \left(\frac{\partial f_{i,0}}{\partial T}\right)\frac{T}{f_{i,0}} \tag{40}$$

$$H_T = \left(\frac{\partial h_{i,0}}{\partial T}\right)\frac{T}{h_{i,0}} \tag{41}$$

$$F_\rho = \left(\frac{\partial f_{i,0}}{\partial \rho}\right)\frac{\rho}{f_{i,0}} \tag{42}$$

$$H_\rho = \left(\frac{\partial h_{i,0}}{\partial \rho}\right)\frac{\rho}{h_{i,0}} \tag{43}$$

$$H_{n_i} = \left(\frac{\mathrm{d}h_x}{\mathrm{d}n_i}\right)\frac{N^t}{h_x} \tag{44}$$

$$F_{n_i} = \left(\frac{\mathrm{d}f_x}{\mathrm{d}n_i}\right)\frac{N^t}{f_x} \tag{45}$$

According to eq 19, the compressibility factors for the reference and the target fluid must be equal. As a result, eq 32 imposes a constraint,

$$z_0 H_\rho = -u_0 F_\rho \tag{46}$$

To calculate the thermodynamic properties mentioned above, the factors H_x and F_x ($x = T$, ρ, n_i) must be known. The derivatives of H are given by Ely,[14]

$$H_\rho = \frac{[(\kappa_i - \kappa_o)u_0]}{[(\kappa_0 - 1)u_0 + (\gamma_0 - 1)z_0]} \tag{47}$$

$$H_T = \frac{[(\gamma_i - \gamma_0)u_0 - (\gamma_0 - 1)(u_i - u_0)]}{[(\kappa_0 - 1)u_0 + (\gamma_0 - 1)z_0]} \tag{48}$$

in which

$$\gamma = \frac{T}{P}\left(\frac{\partial P}{\partial T}\right)_\rho \tag{49}$$

dx.doi.org/10.1021/jp508357f | J. Phys. Chem. B 2014, 118, 14397−14409

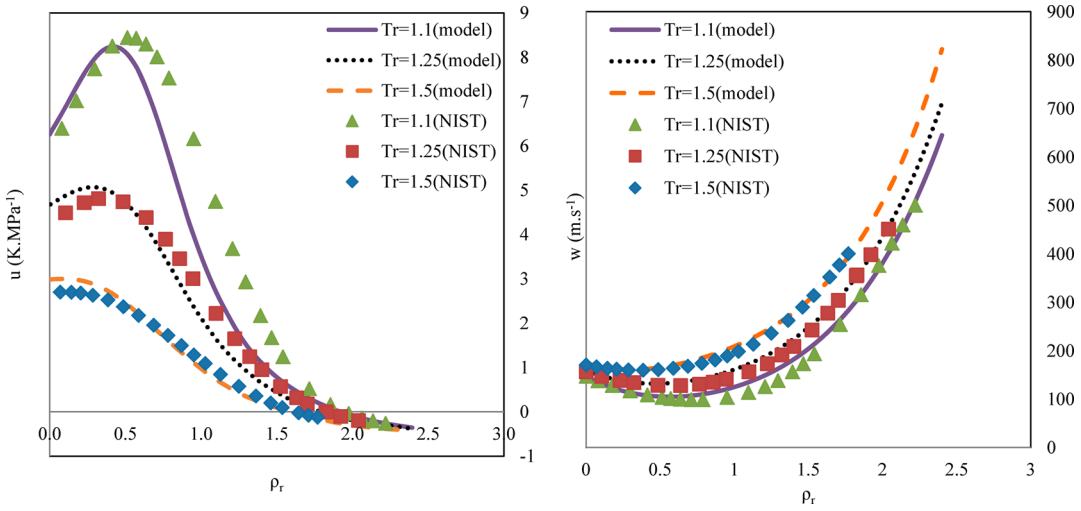

Figure 8. Derived thermodynamic properties for sulphurhexafluoride by the Schmidt−Wagner EoS and comparison with NIST[16] data at different reduced temperatures.

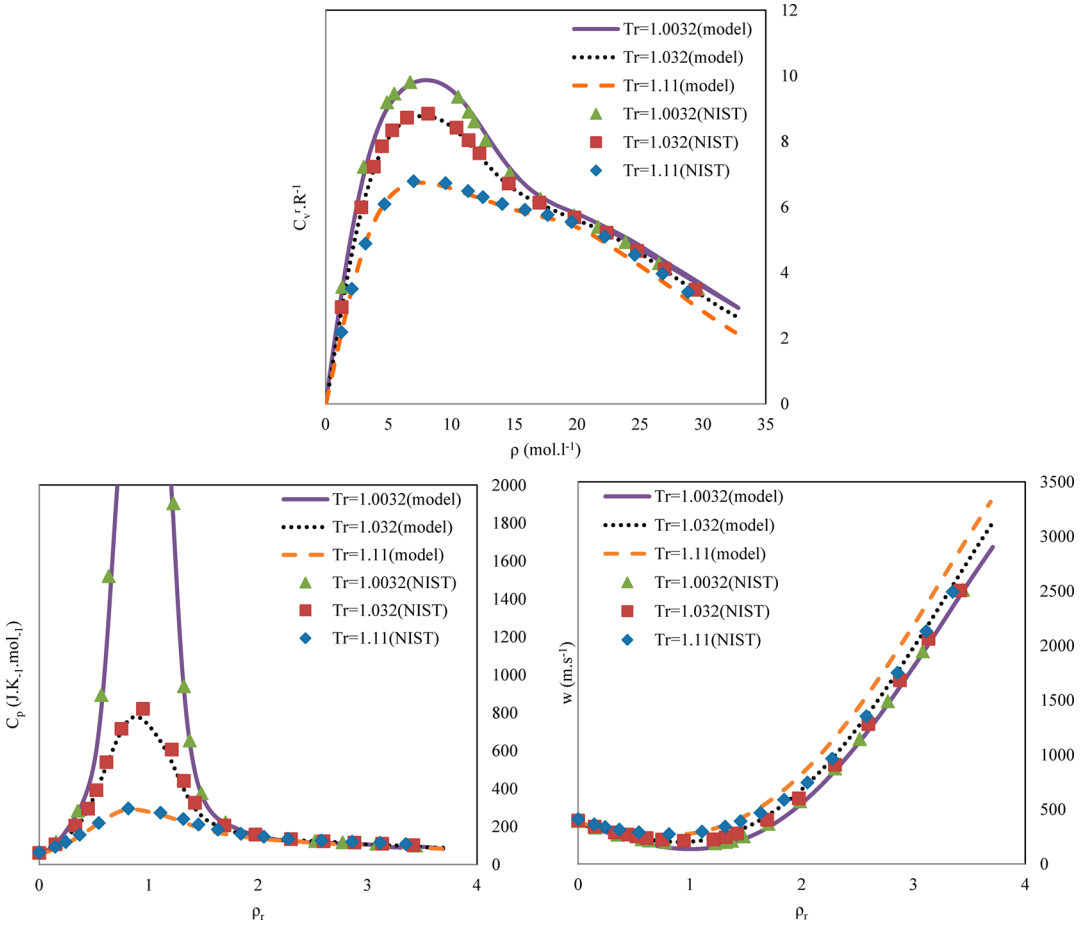

Figure 9. Derived thermodynamic properties for methanol by the Schmidt−Wagner EoS and comparison with NIST[16] data at different reduced temperatures.

$$\kappa = \frac{\rho}{P}\left(\frac{\partial P}{\partial \rho}\right)_T \tag{50}$$

Making use of eqs 33 and 46 allows for the calculation of the F factors. If the aim is to calculate the thermodynamic properties for a mixture, mixing rules are utilized to calculate the mixture factors H_x and F_x. These mixing rules are derived from eqs 27−30,

$$\frac{\mathrm{d}h_{x,0}}{\mathrm{d}T} = \sum_i \sum_j x_i x_j \left(\frac{\mathrm{d}h_{ij,0}}{\mathrm{d}T}\right) \tag{51}$$

dx.doi.org/10.1021/jp508357f | J. Phys. Chem. B 2014, 118, 14397−14409

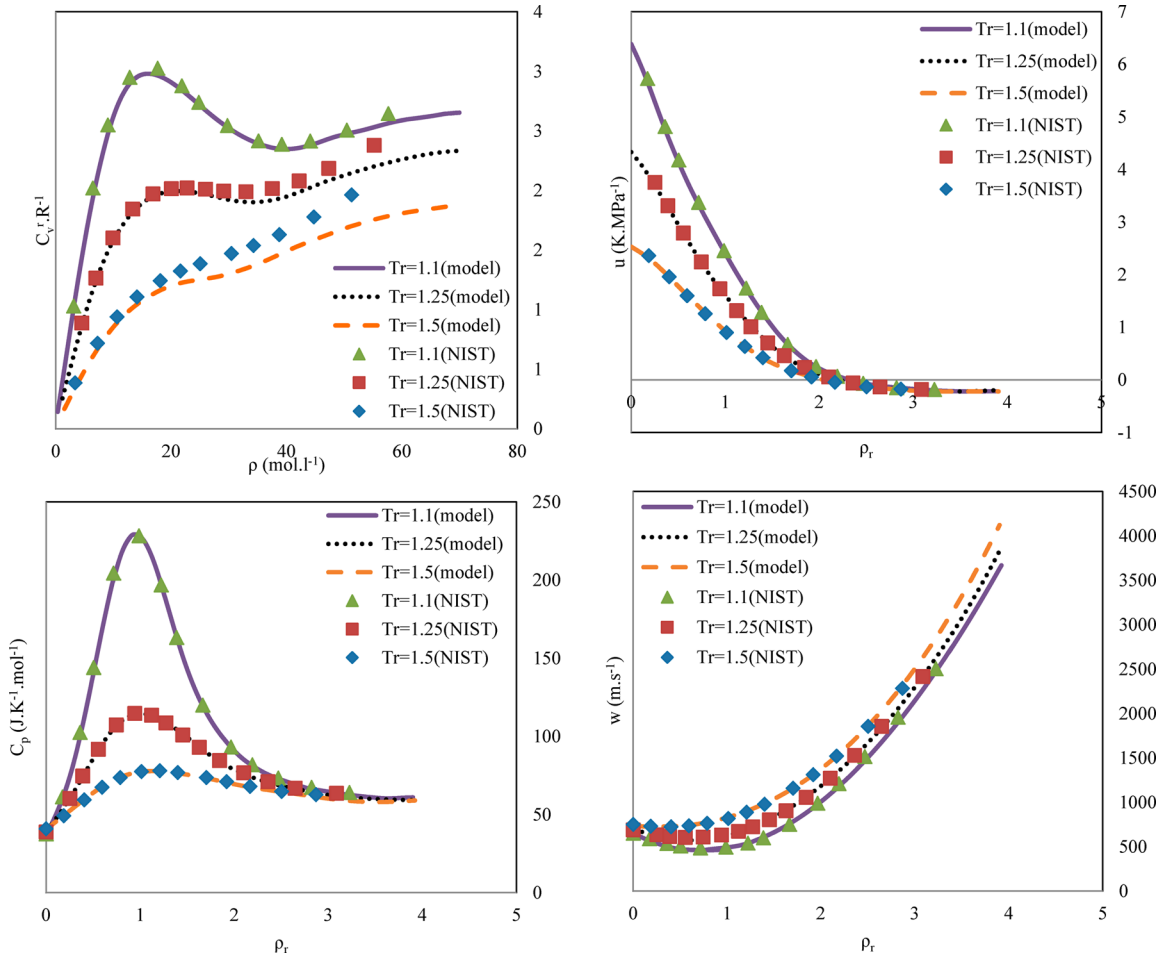

Figure 10. Derived thermodynamic properties for water by the Schmidt−Wagner EoS and comparison with NIST[16] data at different reduced temperatures.

where

$$\frac{dh_{ij,0}}{dT} = \eta_{ij}\frac{1}{8}(h_{i,0}^{1/3} + h_{j,0}^{1/3})^2\left(h_{i,0}^{-2/3}\frac{dh_{i,0}}{dT} + h_{j,0}^{-2/3}\frac{dh_{j,0}}{dT}\right) \quad (52)$$

$$\frac{df_{x,0}}{dT} = \frac{1}{h_{x,0}}\left(\sum_i\sum_j x_i x_j\left(\frac{df_{ij,0}}{dT}h_{ij,0} + f_{ij,0}\frac{dh_{ij,0}}{dT}\right) - f_{x,0}\frac{dh_{x,0}}{dT}\right) \quad (53)$$

$$\frac{df_{ij,0}}{dT} = \epsilon_{ij}\frac{f_{i,0}\frac{df_{j,0}}{dT} + f_{j,0}\frac{df_{i,0}}{dT}}{2\sqrt{f_{i,0}f_{j,0}}} \quad (54)$$

The calculation of caloric properties is more complicated. Detailed equations of the calculations are provided in the Supporting Information.

3. INVESTIGATED COMPOUNDS

In this study, 10 different compounds were selected in a way to encompass different classes of compounds, including nonpolar hydrocarbons, nonpolar cyclic hydrocarbons, refrigerants, and polar compounds. The selected compounds and the literature references presenting the experimental properties investigated in this study are given in Table 2.

4. RESULTS AND DISCUSSION

4.1. Pure Compounds. On the basis of the equations of state discussed in sections 2.1.1 and 2.1.2, the derived thermodynamic properties were calculated for each compound based on the suitable equation of state. The results of these calculations for isochoric heat capacities, isobaric heat capacities, the Joule−Thomson coefficients, and the speeds of sound are compared with literature values for various hydrocarbons in Figures 1−10 for reduced temperatures up to 1.5. In the case of C_v^r, because no direct data are available, the so-called "experimental" C_v^r/R values were calculated according to eqs 16−18. Because the correlations for C_p^r/R have different errors for the different compounds, these "experimental" C_v^r/R values are not exact in Figures 1−10 and are thus not quite suitable for comparing results. For some of the compounds, the deviations of the models from the reference C_v^r/R can be the result of this shortcoming.

As seen in Figures 1−5, the thermophysical properties of alkanes, from methane to butane (both isobutane and normal butane), were predicted with little deviation from the literature data due to the nonpolar nature of these components. C_v^r/R, is, however, an exception as mentioned above. The Schmidt−Wagner EoS was used to model cyclohexane, as a representative of nonpolar cyclic hydrocarbons. Good predictions were obtained as shown in Figure 6. Among the refrigerants, **R152a** was predicted by the 32MBWR EoS and sulphurhexafluoride was predicted by the Schmidt−Wagner EoS, as shown in Figures 7

dx.doi.org/10.1021/jp508357f | J. Phys. Chem. B 2014, 118, 14397−14409

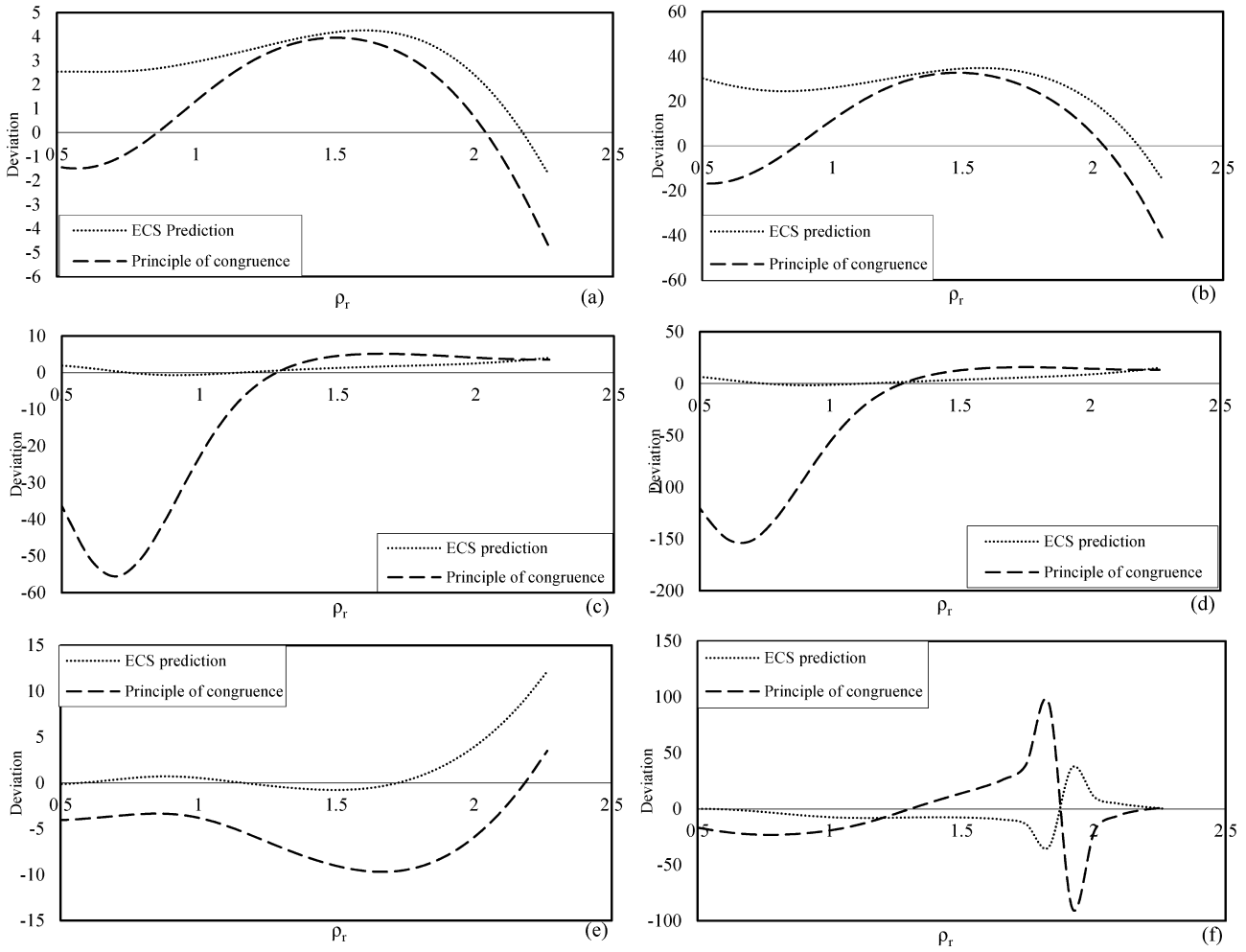

Figure 11. Deviations between the ECS theory and the principle of congruence from the reference surface for calculation of isochoric heat capacity, C_v (a); residual isochoric heat capacity, $C_v^r \cdot R^{-1}$ (b); isobaric heat capacity, C_p (c); residual isobaric heat capacity, $C_p^r \cdot R^{-1}$ (d); speed of sound, w (e); and Joule−Thomson coefficient, μ (f) for the mixture of (x) methane + $(1 - x)$ ethane $(x = 0.685)$ at the temperature of 330 K.

and 8, respectively. While **R152a** was predicted very well, sulphurhexafluoride exhibited large deviations from the data. For the hydrogen-bonding compounds of methanol and water, the Schmidt−Wagner EoS was used with rather accurate predictive capability up to reduced temperatures of 1.1 for methanol and 1.5 for water, as shown in Figures 9 and 10, respectively.

In almost all of the compounds investigated, the velocity of sound showed the most accurate EoS-predicted results compared to the other derivative physical properties (Figures 1−10). The velocity of sound has an ascending trend in all of the cases with respect to reduced density. Isochoric heat capacity, isobaric heat capacity, and the Joule−Thomson coefficient all show maxima in the investigated density range, with the Joule−Thomson coefficient of water being an exception.

4.2. Evaluation of the Accuracies of the ECS Calculations. To further investigate the derivative properties obtained from models, the ECS theory was also extended to analytically predict the derivative properties of mixtures. The advantage of the ECS procedure is the high accuracy of the predictions and the ability to predict the properties for an infinite number of mixtures. The results from ECS calculations are compared to properties derived from a constant-composition reference surface given by McCarty.[13] The mixture considered is methane + ethane, with a molar fraction of methane equal to 0.685. The critical density of the mixture is 8.82 mol·L^{-1}. All calculations are carried out for a temperature of 330 K. The accuracy of the ECS calculations can be observed using Figure 11. In all of the graphs of Figure 11, deviations of the ECS theory from the reference surface have been shown for the derivative properties considered, with the deviations being defined as

$$\Delta = \frac{(X_{\text{reference}} - X_{\text{test}}) \times 100}{X_{\text{reference}}} \tag{55}$$

where X is the derivative property of concern. The interaction parameters are set to 1.0. The properties from the constant-composition reference surface are also compared in Figure 11 to those given by the principle of congruence, which states that, for nonpolar, approximately spherical molecules, the properties for the mixture are the molar fraction-weighted sum of the pure component properties at the same density and temperature.

For the isochoric heat capacity, seen in Figure 11a, the predictions given by the principle of congruence are generally better than those by ECS calculations. This could be a result of an unsatisfactory reference equation of state, as well as of the inadequacy of the ECS theory. Figure 11b is basically a similar comparison as the one given in Figure 11a, but the ideal heat capacity has been subtracted to give a comparison of the residual heat capacities. It is evident that deviations in the residual isochoric heat capacities are large. In Figure 11c, a comparison

dx.doi.org/10.1021/jp508357f | J. Phys. Chem. B 2014, 118, 14397−14409

between isobaric heat capacities is presented. The principle of congruence gives huge deviations in the critical region. The ECS calculations give deviations less than 5% in the whole range of densities. The residual isobaric heat capacities, presented in Figure 11d, indicate that the predicted total isobaric heat capacity calculated with the ECS procedure resulted in deviations of less than 5% in the whole density range. The deviations of the principle of congruence are much larger than ECS predictions, but close to the critical point, they reach up to almost 20%. The deviations in the speed of sound are given in Figure 11e. The predictions given by the ECS calculations have deviations of less than 5 % in the whole reduced density range up to 2, above which the pure component surfaces used in the ECS calculation are probably not accurate. For the Joule–Thomson coefficient (Figure 11f), again the ECS predictions prove to be superior to the calculations using the principle of congruence.

For a further investigation of the ECS procedure, the measured isobaric heat capacities are compared to the ECS predictions, also for a binary system. Figures 12 and 13 show the estimations,

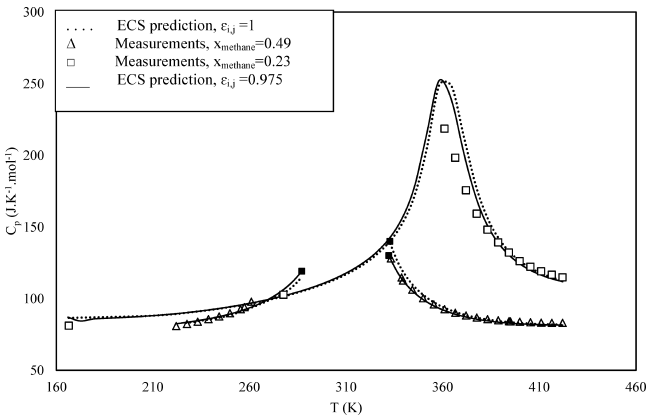

Figure 12. Predicted and experimental isobaric heat capacities for mixtures of methane + propane at a pressure of 6.89 MPa (saturation temperatures = ■).

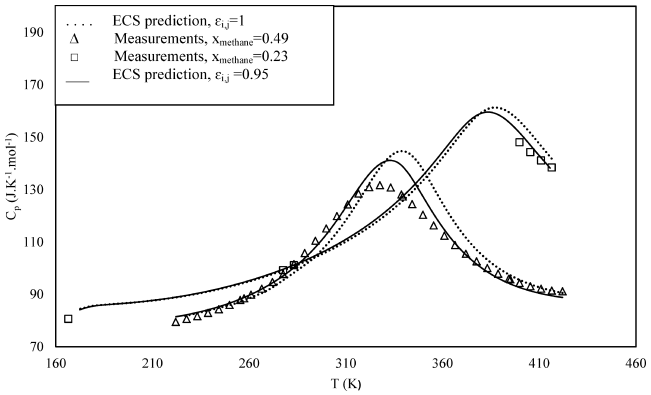

Figure 13. Predicted and experimental isobaric heat capacities for mixtures of methane + propane at a pressure of 10.34 MPa.

together with the experimental data of methane + propane, taken from Yesavage[17] at two different pressures and two concentrations. At a methane molar concentration of 0.23, the experimental mixture critical pressure, temperature, and density were measured to be 6.21 MPa, 353.40 K, and 5.560 mol·L^{-1}, respectively, and for a methane molar concentration of 0.49, the mixture critical properties were 8.50 MPa, 325.17 K, and 7.105 mol·L^{-1}, respectively.

In Figure 12, plotted for a pressure of 6.89 MPa, the isobaric heat capacities obtained with the ECS procedure by setting all interaction parameters equal to 1 are quite satisfactory, away from the critical region. There is, however, significant error near the critical point. An effort has been made to correct the deviations by optimizing the interaction parameter. With the optimized value of $\varepsilon_{i,j}$ = 0.975 (eq 27), better representations of the data below the critical point were obtained. The deviations above the critical point, however, were not eliminated. Such errors may be due to the failure of the pure component surfaces to give a good representation of the derived properties in the immediate vicinity of the critical point.

Similar results are found for this system at a higher pressure of 10.34 MPa (Figure 13), since here too it is not possible to reach an accurate representation of the data close to the critical temperature, even by adjusting the interaction parameter ε_{ij}. To obtain a reasonable representation, the interaction parameter was optimized to 0.95.

5. CONCLUSIONS

In this study, the behavior of the isochoric heat capacity, isobaric heat capacity, speed of sound, and Joule–Thomson coefficient for pure compounds and mixtures were investigated based on the 32-MBWR and SW equations of state. The accuracy of these two models were found to be comparable in predicting the above-mentioned derivative properties. The SW EoS is better in representing the derivative properties in the critical region; however, it is more complex than the 32-MBWR. The 32-MBWR is a more popular EoS in the literature (with respect to SW EoS), perhaps because of its more straightforward equations and programming. This is, of course, a great advantage when writing a computer code for the calculation of derivative properties. If more accurate representations of derivative properties are required in the critical region, then the SW EoS is the better choice. The 32-MBWR EoS is recommended for derivative property predictions of nonpolar hydrocarbons, whereas the SW EoS seems to be the more suitable choice for the nonpolar cyclic hydrocarbons and the polar compounds investigated in this study.

In addition, to compare the ECS procedure and the principle of congruence for mixtures of components, the mixture of methane + propane has been investigated and the isochoric heat capacities, residual isochoric heat capacities, isobaric heat capacities, residual isobaric heat capacities, speeds of sound, and Joule–Thomson coefficients were calculated by these two different methods. It was shown that the ECS procedure is more accurate compared to the principle of congruence for this system.

■ ASSOCIATED CONTENT

Supporting Information

Detailed equations of the calculations of caloric properties. This material is available free of charge via the Internet at http://pubs.acs.org.

■ AUTHOR INFORMATION

Corresponding Author

*E-mail: cpeters@pi.ac.ae.

Notes

The authors declare no competing financial interest.

■ ACKNOWLEDGMENTS

We would like to thank Daniel G. Friend at NIST in Boulder (Colorado) for providing heat capacity data on mixtures of methane + propane. Also, S.R. is thankful to Prof. Maaike Kroon and to Shiraz University and Eindhoven University of Technology for facilitating this joint research.

■ NOMENCLATURE

A Helmholtz energy (J/mol)
a dimensionless residual Helmholtz energy
b co-volume in cubic equations of state (L mol^{-1})
C_p isobaric heat capacity ($J{\cdot}K^{-1}{\cdot}mol^{-1}$)
C_p^r residual isobaric heat capacity ($J{\cdot}K^{-1}{\cdot}mol^{-1}$)
C_v isochoric heat capacity ($J{\cdot}K^{-1}{\cdot}mol^{-1}$)
C_v^r residual isochoric heat capacity ($J{\cdot}K^{-1}{\cdot}mol^{-1}$)
h transformation parameter (ECS)
f transformation parameter (ECS)
M_r molar mass (g mol^{-1})
P pressure (MPa)
R gas constant ($J{\cdot}K^{-1}{\cdot}mol^{-1}$)
S entropy ($J{\cdot}K^{-1}{\cdot}mol^{-1}$)
T absolute temperature (K)
x_i mole fraction of component i
Z compressibility factor
U residual compressibility factor ($J{\cdot}mol^{-1}$)
w speed of sound ($m{\cdot}s^{-1}$)

Greek

ω Pitzers acentric factor
ρ_r reduced density
ρ density ($mol{\cdot}L^{-1}$)
μ Joule−Thomson coefficient ($K{\cdot}MPa^{-1}$)
θ shape factor (ECS)
ϕ shape factor (ECS)
ε_{ij} binary interaction parameter (ECS)
η_{ij} binary interaction parameter (ECS)
ϕ_i fugacity

Indices

r reduces properties
c critical properties
id ideal gas state
i target fluid

■ REFERENCES

(1) Keshtkari, S.; Haghbakhsh, R.; Raeissi, S.; Florusse, L.; Peters, C. J. Vapor−Liquid Equilibria of Isopropyl Alcohol + Propylene at High Pressures: Experimental Measurement and Modelling with The CPA EoS. *J. Supercrit. Fluids* **2013**, *84*, 182−189.

(2) Maghari, A.; Hamzehloo, M. Second-Order Thermodynamic Derivative Properties of Binary Mixtures of *n*-Alkanes through the SAFT-CP Equation of State. *Fluid Phase Equilib.* **2011**, *302*, 195−201.

(3) Llovell, F.; Peters, C. J.; Vega, L. F. Second-Order Thermodynamic Derivative Properties of Selected Mixtures by the Soft-SAFT Equation of State. *Fluid Phase Equilib.* **2006**, *248*, 115−122.

(4) Shin, M. S.; Lee, Y.; Kim, H. Estimation of Second-Order Derivative Thermodynamic Properties Using the Crossover Cubic Equation of State. *J. Chem. Thermodyn.* **2008**, *40*, 688−694.

(5) Llovell, F.; Vega, L. F. Prediction of Thermodynamic Derivative Properties of Pure Fluids through the Soft-SAFT Equation of State. *J. Phys. Chem. B* **2006**, *110*, 11427−11437.

(6) Gregorowicz, J.; O'Connell, J. P.; Peters, C. J. Some Characteristics of Pure Fluid Properties that Challenge Equation of State Models. *Fluid Phase Equilib.* **1996**, *116*, 94−101.

(7) de Villiers, A. J.; Schwarz, C. E.; Burger, A. J.; Kontogeorgis, G. M. Evaluation of the PC-SAFT, SAFT and CPA Equations of State in Predicting Derivative Properties of Selected Non-Polar and Hydrogen-Bonding Compounds. *Fluid Phase Equilib.* **2013**, *338*, 1−15.

(8) Forte, E.; Llovell, F.; Trusler, J. P. M.; Galindo, A. Application of the Statistical Associating Fluid Theory for Potentials of Variable Range (SAFT-VR) Coupled with Renormalisation-Group (RG) Theory to Model the Phase Equilibria and Second-Derivative Properties of Pure Fluids. *Fluid Phase Equilib.* **2013**, *337*, 274−287.

(9) Lundstrøm, C.; Michelsen, M. L.; Kontogeorgis, G. M.; Pedersen, K. S.; Sørensen, H. Comparison of the SRK and CPA Equations of State for Physical Properties of Water and Methanol. *Fluid Phase Equilib.* **2006**, *247*, 149−157.

(10) Schmidt, R.; Wagner, W. A New Form of the Equation of State for Pure Substances and its Application to Oxygen. *Fluid Phase Equilib.* **1985**, *19*, 175−200.

(11) Jacobsen, R. T.; Stewart, R. B. Thermodynamic Properties of Nitrogen Including Liquid and Vapour Phases from 63 to 2000 K with Pressures to 10,000 bar. *J. Phys. Chem. Ref. Data* **1973**, *2*, 757−922.

(12) Poling, B. E.; Prausnitz, J. M.; O'Connell, J. P. *The Properties of Gases and Liquids*, 5th ed.; McGraw-Hill: New York, 2000; pp 745−760.

(13) McCarty, R. D. Extended Corresponding States as a Tool for the Prediction of the Thermodynamic Properties of Mixtures. *Int. J. Thermophys.* **1986**, *7*, 901−910.

(14) Ely, J. F. A Predictive, Exact Shape Factor Extended Corresponding States Model for Mixtures. *Adv. Cryog. Eng.* **1990**, *35*, 1511−1520.

(15) Noro, M. G.; Frenkel, D. Extended Corresponding-States Behavior for Particles with Variable Range Attractions. *J. Chem. Phys.* **2000**, *113*, 2941−2945.

(16) *NIST Chemistry WebBook*; NIST Standard Reference Database Number 69; Linstrom, P. J., Mallard, W. G., Eds.; National Institute of Standards and Technology: Gaithersburg, MD; http://webbook.nist.gov (accessed August 19, 2013).

(17) Yesavage, V. F. The Measurement and Prediction of the Enthalpy of Fluid Mixtures Under Pressure. Ph.D. thesis, Department of Chemical and Metallurgical Engineering, The University of Michigan, 1968.